The Dynamics of Hamiltonian Lattices With Application to Hollomon Oscillators

Aigerim Zholmaganbetova

Master of Science Thesis in Applied Mathematics

Department of Mathematics, School of Science and Technology
Nazarbayev University
Astana 010000, Kazakhstan
azholmaganbetova@nu.edu.kz

MSc Thesis Supervisor: Professor Anastasios Bountis

Members of Examination Committee:

Assist. Prof. Ardak Kashkynbaev
Department of Mathematics
School of Science and Technology
Nazarbayev University

Assist. Prof. Thomas Oikonomou
Department of Physics
School of Science and Technology
Nazarbayev University

Research Assist. Prof. Nikos Lazarides
Department of Physics
University of Crete, Greece

DEPARTMENT OF MATHEMATICS, NAZARBAYEV UNIVERSITY
KABANBAY BATYR 53, NUR-SULTAN, 010000, REPUBLIC OF KAZAKHSTAN
MAY 2019

Abstract

Many problems in theoretical physics are expressed in the form of Hamiltonian systems. Among these the first to be extensively studied were low-dimensional, possessing as few as two (or three) degrees of freedom. In the last decades, however, great attention has been devoted to Hamiltonian systems of high dimensionality. The most famous among them are the ones that deal with the dynamics and statistics of a large number N of mass particles connected with nearest neighbor interactions. At low energies E, these typically execute quasiperiodic motions near some fundamental stable periodic orbits (SPOs) which represent nonlinear continuations of the N normal mode solutions of the corresponding linear system. However, as the energy is increased, these solutions destabilize causing the motion in their vicinity to drift into chaotic domains, thus giving rise to important questions concerning the systems behavior in the thermodynamic limit, where E and N diverge with $E/N = constant$. One of the open problems in Hamiltonian dynamics, therefore, examines the relation between local (linear) stability properties of simple periodic solutions of Hamiltonian systems, and the more "global" dynamics. In this thesis, after reviewing the main results on these topics for the case of N-particle Fermi-Pasta-Ulam Hamiltonians, I proceed to apply the corresponding methods to a lattice of Hollomon oscillators, which are of interest to applications in problems of nonlinear elasticity.

ACKNOWLEDGEMENTS

Firstly, I would like to express my sincere gratitude to my advisor Prof. Anastasios Bountis for the continuous support of my Master's Thesis study and related research, for his patience, motivation, and immense knowledge.

During this research, I had collaborations with several members of Prof. A. Bountis research team to make my work more efficient. Professor Bountis shared his valuable experience and regularly discussed with MSc students under his guidance the derivations and every time helped to turn to the next stage. Moreover, Professor's international collaborators helped me better understand the tasks involved in this project like Prof. Thomas Oikonomou and Nikos Lazarides. They taught me how to construct and implement Matlab codes for such tasks.

Also, I would like to emphasize the help of studies during second Summer School of Kazakhstan on "Mathematical Methods in Science and Technology", which held on May 28-June 8, 2018, at the campus of the Al Farabi Kazakh National University in Almaty.

Besides my advisor, I would like to thank the rest of the thesis committee, for their insightful comments and encouragement during preparations, but also for the hard questions which incented me to widen my research from various perspectives.

Last but not the least, I would like to thank my family: my parents and my brother and sister for supporting me spiritually throughout writing this thesis and my life in general.

CONTENTS

I. INTRODUCTION

A. The case of $N = 1$ degree of freedom

Hamiltonian lattice dynamical systems produce exceptional group of models in all parts of natural sciences. They are helpful in researching such aspects as solid state physics, use of several oscillators in engineering, molecular biology, etc. There are many things to discover about the properties and nature of lattice dynamical systems. They can be imagined as a big combination of moving molecules or pieces. In mathematics, they are defined as a enormous number (finite or infinite) of ordinary differential equations (ODE) [5].

In this MSc thesis we intend to study a special class of Hamiltonian dynamical systems of N degrees of freedom (dof), evolving in an $n-$dimensional phase space of position and momentum coordinates $q_k(t)$, $p_k(t)$ respectively, $k = 1, 2, ..., N$, with $n = 2N$, whose equations of motion are

$$\frac{dq_k}{dt} = \frac{\partial H}{\partial p_k}, \frac{dp_k}{dt} = -\frac{\partial H}{\partial q_k}, k = 1, 2, ..., N \tag{1}$$

where H is the Hamiltonian function [11]. Since we assume in (1) that H does not explicitly depend on time t, H is a first integral of the motion and its value E equals the total energy of the system. We also assume that H can be expanded in power series as a sum of homogeneous polynomials H_m of degree $m \geq 2$.

$$\begin{aligned} H &= H_2(q_1, ..., q_N, p_1, ..., p_N) \\ &+ H_3(q_1, ..., q_N, p_1, ..., p_N) + ... \\ &= E \end{aligned} \tag{2}$$

so that the origin $q_k(t) = p_k(t) = 0$, is an equilibrium point of the system. Thus, $H = E$ defines a $(2N-1)$ dimensional complex called the (constant) energy surface, on which the dynamics expands. We accept that making equations (1) linear with respect to the origin generates a matrix, whose eigenvalues arise in conjugate imaginary pairs, $\pm i\omega k$, $k = 1, ..., N$, providing the N frequencies of the normal mode oscillations of the linear problem. Then, according to a famous theorem by Lyapunov [22], if there are no integers among eigenvalues $\frac{\omega_j}{\omega_k}$, for any $j, k = 1, 2, ..., N$, where $j \neq k$, then the linear normal modes persist to occur as periodic solutions of the nonlinear problem, with frequencies close to those of the linear modes and can be presented as examples of $simple\ periodic\ orbits$ (SPOs) of the system oscillating with the same frequency. Introduction of the spectrum of Lyapunov exponents, shows us how its properties are connected to the emergence of strongly (large scale) chaotic behavior in the solutions [21], [31].

One of the first physical systems bore in this group is the harmonic oscillator. It characterizes the oscillations of a mass m on a spring, which applies on the mass a force that is proportional to the negative of the displacement q of the mass from its equilibrium position ($q = 0$), as shown in Fig. 1. The dynamics is described by Newton's second order differential equation

$$m\frac{d^2q}{dt^2} = -kq, \tag{3}$$

where $k > 0$ is a constant representing the hardness (or softness) of the spring [5]. Equation (3) can be easily solved by standard techniques of linear ODEs to yield the displacement $q(t)$ as an oscillatory function of time of the form

$$q(t) = Asin(\omega t + \alpha), \omega = \sqrt{k/m}, \tag{4}$$

where A and α are free constants corresponding to the amplitude and phase of oscillations and ω is the frequency.

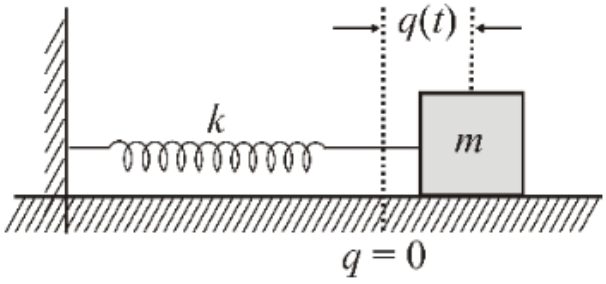

Fig. 1. A harmonic oscillator consists of a mass m moving horizontally on a frictionless table under the action of a force which is proportional to the negative of the displacement $q(t)$ of the mass from its equilibrium position at $q = 0$ ($k > 0$ is a proportionality constant).

We anticipate that the dynamics is derived from the Hamiltonian function

$$H(q,p) = \frac{p^2}{2m} + k\frac{q^2}{2} = E, \tag{5}$$

which is an integral of the motion (since $\frac{\partial H}{\partial t} = 0$), whose value E represents the total (kinetic plus potential) energy of the system.

Thus, if we consider a Hamiltonian system of $N = 1$ dof, as a mass-spring system, without attempting to solve (1), we may study them geometrically as a one-parameter family of trajectories (or orbits) given by (1) and plotted in the (q, p) phase space of the system in Fig. 2. Thus, analogous to what this figure shows, there are, in $N > 1$ degress of freedom, central points, like the center (0,0) in Fig. 2, around which $q(t)$ and $p(t)$ oscillate periodically with the same frequency ω. In such higher dimensional models, as we find in this thesis, the point (0,0) becoimes the intersection of a Simple Periodic Orbit (SPO) with this surface and the fact that it is surrounded by elliptical orbits means that this SPO is *stable under small perturbations* [23], [30], [32].

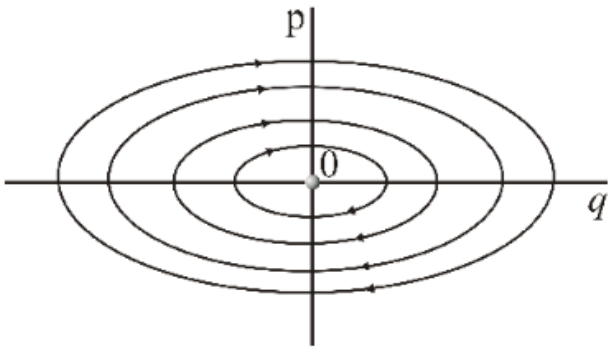

Fig. 2. Plot of the solutions of the harmonic oscillator Hamiltonian function in the (q, p) phase space, as a one-parameter family of curves, for different values of the total energy E.

Let us turn to a more interesting one dof Hamiltonian system representing the motion of a simple pendulum shown in Fig. 3. Its equation of motion according to classical mechanics is

$$\frac{d^2\theta}{dt^2} = -\frac{g}{l}\sin\theta, \tag{6}$$

where the right side of (6) expresses the restoring torque due to the weight mg of the mass (g being the acceleration due to gravity) and the left side describes the time derivative of the angular

momentum of the mass. If we now write this equation as a system of two first order ODEs, as we did for the harmonic oscillator, we find again that they can be cast in Hamiltonian form

$$\frac{dq}{dt} = p = \frac{\partial H}{\partial p}, \quad \frac{dp}{dt} = -\frac{g}{l}\sin q = -\frac{\partial H}{\partial q}, \tag{7}$$

where $q = \theta$ and l is the length of the pendulum. Of course, we cannot solve these equations as easily as we did for the harmonic oscillator. The solution of (7) can be obtained via the so-called Jacobi elliptic functions [11], [18] , which have been thoroughly studied in the literature and are directly related to the solution of an anharmonic oscillator with cubic nonlinearity, about which we will have a lot to say in later sections. Still, we can make great progress in understanding

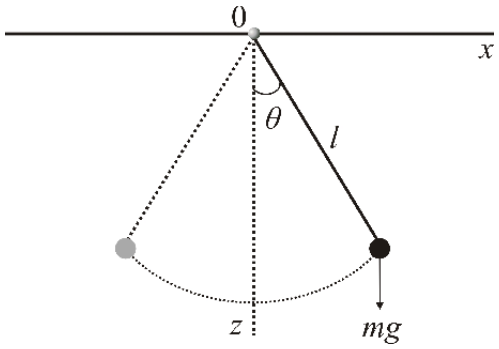

Fig. 3. The simple pendulum is moving in the two-dimensional plane (x, z), but its motion is completely described by the angle θ and its derivative $\partial\theta/\partial t$.

the dynamics of the simple pendulum through its Hamiltonian function, which provides the energy integral

$$H(q,p) = \frac{p^2}{2} + \frac{g}{l}(1 - \cos q) = E. \tag{8}$$

Plotting this family of curves in the (q, p) phase space for different values of E we now obtain a much more interesting picture than Fig.2 depicted in Fig. 4. Observe that, besides the elliptic fixed point at the origin, there are two new equilibria located at the points $(\pm\pi, 0)$. These are called *saddle points* and *repel* most orbits in their neighborhood along hyperbola-looking trajectories. For this reason points A and B in Fig. 4 are also called *unstable*, in contrast to the $(0, 0)$ fixed point, which is called *stable*. More precisely, in view of the theory presented in Chap. I, $(0, 0)$ is characterized by what we called conditional (or neutral) stability.

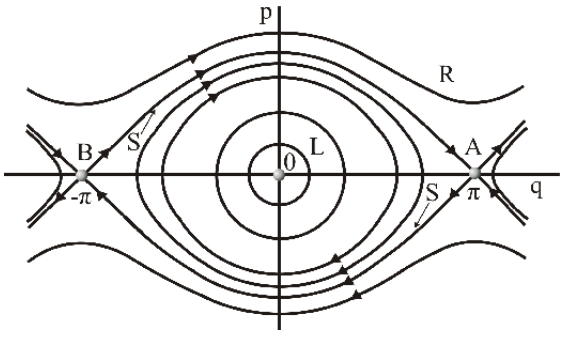

Fig. 4. Plot of the curves of the energy integral (8) in the (q, p) phase space. Note, the presence of additional equilibrium points at $(\pm\pi, 0)$, which are of the saddle type. Observe also the curve S separating oscillatory motion (L) about the central elliptic point at $(0, 0)$ from rotational motion (R).

B. The case of $N = 2$ degrees of freedom

Following the above discussion, it would be natural to extend our study to Hamiltonian systems of two dof, joining at first two harmonic oscillators, as shown in Fig. 5 and applying the approach of Sect. I-A. We furthermore assume that our oscillators have equal masses $m_1 = m_2 = m$ and spring constants $k_1 = k_2 = k$ and impose fixed boundary conditions to their endpoints, as shown in Fig. 5. Clearly, Newton's equations of motion give in this case:

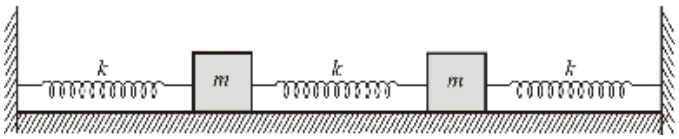

Fig. 5. Two coupled harmonic oscillators of equal mass m and force constant k, with displacements $q_1(t)$, $q_2(t)$ from their equilibrium position, moving horizontally on a frictionless table with their endpoints firmly attached to two immovable walls.

$$m\frac{d^2q_1}{\partial t^2} = -kq_1 - k(q_1 - q_2), \quad m\frac{d^2q_2}{\partial t^2} = -kq_2 + k(q_1 - q_2), \tag{9}$$

where $q_i(t)$ are the particles' displacements from their equilibrium positions at $q_i = 0$, $i = 1, 2$. If we also introduce the momenta $p_i(t)$ of the two particles in terms of their velocities, as we did for the single harmonic oscillator, we arrive at the following fourth order system of ODEs

$$\frac{dq_1}{dt} = \frac{p_1}{m}, \quad \frac{dp_1}{\partial t} - kq_1 - k(q_1 - q_2), \quad \frac{dq_2}{\partial t} = \frac{p_2}{m}, \quad \frac{dp_2}{dt} - kq_2 + k(q_1 - q_2), \tag{10}$$

which is definitely Hamiltonian, since it is derived from the Hamiltonian function

$$H(q_1, p_1, q_2, p_2) = \frac{p_1^2}{2m} + \frac{p_2^2}{2m} + k\frac{q_1^2}{2} + k\frac{q_2^2}{2} + k\frac{(q_1 - q_2)^2}{2} = E \tag{11}$$

expressing the integral of total energy E. Note that we may think of the two endpoints of the system as represented by positions and momenta q_0, p_0 and q_3, p_3 that vanish identically for all t.

What can we say about the solutions of this system? What would happen, for example, if a *second integral* of the motion were available? Could the method of quadratures lead us to the solution in that case? Is it perhaps possible to use a suitable coordinate transformation to separate them and write our equations as a system of two uncoupled harmonic oscillators?

It is not very difficult to answer this question. Indeed, if we perform the change of variables

$$Q_1 = \frac{q_1 + q_2}{\sqrt{2}}, \quad Q_2 = \frac{q_1 - q_2}{\sqrt{2}}, \quad P_1 = \frac{p_1 + p_2}{\sqrt{2}}, \quad P_2 = \frac{p_1 - p_2}{\sqrt{2}} \tag{12}$$

(the factor $1/\sqrt{2}$ will be explained later), we see that, adding and subtracting by sides the two equations in (9) (dividing also by m and introducing $\omega = \sqrt{k/m}$), splits the problem to two harmonic oscillators

$$\frac{\partial Q_i}{\partial t} = \frac{P_i}{m}, \quad \frac{\partial P_i}{\partial t} = -\omega_i^2 Q_i, \quad i = 1, 2, \quad \omega_1 = \omega, \quad \omega_2 = \sqrt{3}\omega, \tag{13}$$

which have *different* frequencies ω_1, ω_2. Observe that the new Hamiltonian of the system becomes

$$K(Q_1, P_1, Q_2, P_2) = \frac{P_1^2}{2m} + \frac{P_2^2}{2m} + k\frac{Q_1^2}{2} + 3k\frac{Q_2^2}{2} = E. \tag{14}$$

We now see that the factor $1/\sqrt{2}$ was introduced in (12) to make the new equations of motion (13) have the same *canonical form* as two uncoupled harmonic oscillators, while the new Hamiltonian K is expressed as the sum of the Hamiltonians of these oscillators. In this way, we may say that changing from q_i, p_i to Q_i, P_i variables we have performed a canonical coordinate transformation to our system.

In this framework, we immediately realize that our problem possesses not one but *two* integrals of the motion which may be thought of as the energies of the two oscillators

$$F_i(Q_1, P_1, Q_2, P_2)) = \frac{P_i^2}{2m} + k_i \frac{Q_i^2}{2} = E_i, \quad i = 1, 2, \tag{15}$$

with $k_1 = k$, $k_2 = 3k$, while E_i are two free parameters of the system to be fixed by the initial conditions $q_i(0)$, $p_i(0)$, $i = 1, 2$. Thus, we may now proceed to apply the method of quadratures to each of these oscillators, as described in Sect. I-A to obtain the general solution of the system in the form

$$Q_i(t) = \sqrt{\frac{2E_i}{k_i}} \sin(\omega_i(t + c_i)), \quad i = 1, 2, \tag{16}$$

c_i being the other two free parameters needed for the complete solution of the 4 first order ODEs (13). Naturally, if we wish to write our general solution in terms of the original variables of the problem, we only need to invert equations (12) to find $q_1(t)$, $q_2(t)$. We also remark that the above considerations show that the only fixed point of the system lies at the origin of phase space and is elliptic (why?)

Let us make a crucial observation at this point: The above analysis shows that, for a system of 2 dof, 2 integrals are necessary and sufficient for its integration by quadratures, as the remaining two arbitrary constants c_1, c_2 merely represent phases of oscillation and are not as important as E_1 and E_2. To understand this better, note that c_1, c_2 are *not* single-valued and hence do not belong to the class of integrals required by the LA theorem for complete integrability.

All this suggests that it would be advisable to introduce one more transformation to the so-called *action-angle* variables $I_i, \theta_i,\ i = 1, 2$ as follows

$$Q_i = \sqrt{\frac{2\omega_i I_i}{k_i}} \sin\theta_i, \quad P_i = \sqrt{2m\omega_i I_i} \cos\theta_i, \quad i = 1, 2 \tag{17}$$

and write our integrals (15) as $F_i = I_i\omega_i$ so that the new Hamiltonian (14) may be expressed in a form

$$G(I_1, \theta_1, I_2, \theta_2) = G(I_1, I_2) = I_1\omega_1 + I_2\omega_2 \tag{18}$$

that is *independent* of the angles θ_i, which also demonstrates the irrelevance of the phases of the oscillations in (16). Evidently, our action-angle variables also satisfy Hamilton's equations of motion

$$\frac{d\theta_i}{dt} = \frac{\partial G}{\partial I_i} = \omega_i, \quad \frac{dI_i}{dt} = -\frac{\partial G}{\partial \theta_i} = 0, \tag{19}$$

which imply that the new momenta I_i are constants of the motion, while the θ_i are immediately integrated to give $\theta_i = \omega_i t + \theta_{i0}$, where θ_{i0} are the two initial phases. Thus, the change to action-angle variables defines a canonical transformation and the oscillations (17) are called *linear normal modes* of the system.

Let us now discuss the solutions of this coupled system of linear oscillators. Using (12) and (16) we see that they are expressed, in general, as linear combinations of two trigonometric oscillations with frequencies $\omega_1 = \sqrt{k}$, $\omega_2 = \sqrt{3k}$. If these frequencies were *rationally dependent*, i.e. if their ratio were a rational number $\omega_1/\omega_2 = m_1/m_2$ (m_1, m_2 being positive integers with no common divisor) all orbits would *close* on 2-dimensional *invariant tori*, like the one shown in Fig. 6 and the motion would be periodic (what are the m_1, m_2 of the orbit shown in Fig. 6?). Note that in our example, this could only happen for initial conditions such that E_1 or E_2 is zero, whence the solutions would execute in-phase or out-of-phase oscillations with frequency ω_2, or ω_1 respectively.

In the general case, though, E_1 and E_2 are both non-zero and the oscillations are *quasiperiodic*, in the sense that they result from the superposition of trigonometric terms whose frequencies are *rationally independent*, as the ratio $\omega_2/\omega_1 = \sqrt{3}$ is an irrational number. Hence, the orbits produced by these solutions in the 4-dimensional phase space are *never closed* (periodic). Unlike the orbit shown in Fig. 6, they never pass by the same point, covering eventually uniformly the 2-dimensional torus of Fig. 6 specified by the values of E_1 and E_2.

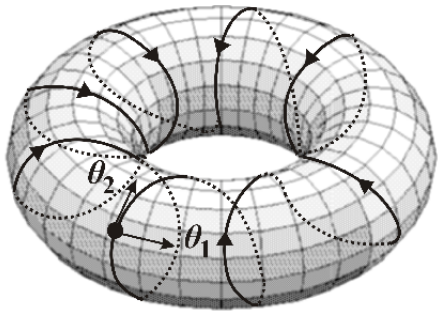

Fig. 6. If the ratio of the frequencies of a 2 dof integrable Hamiltonian system is a *rational* number, the orbits are periodic (and hence close upon themselves) on 2-dimensional invariant tori, such as the one shown in the figure. However, if the ratio ω_1/ω_2 is irrational, the orbits never close and eventually cover uniformly 2-dimensional tori in the 4-dimensional phase space of the coordinates q_i, p_i, $i = 1, 2$.

Let us now turn to the case of a system of two coupled *nonlinear* oscillators. In particular, we shall discuss here one of the most famous Hamiltonian 2 dof systems, originally due to Hénon and Heiles [17]

$$H = \frac{1}{2m}(p_1^2 + p_2^2) + \frac{1}{2}(\omega_1^2 q_1^2 + \omega_2^2 q_2^2) + q_1^2 q_2 - \frac{C}{3} q_2^3. \tag{20}$$

This describes the motion of a star of mass m in the axisymmetric potential of a galaxy whose lowest order (quadratic) terms are those of two uncoupled harmonic oscillators and the only higher order terms present are cubic in the q_1, q_2 variables (for a most informative recent review on the applications of nonlinear dynamics and chaos to galaxy models see [10]). Note that the value of m in (20) can be easily scaled to unity by appropriately rescaling time, while an additional parameter before the $q_1^2 q_2$ term in (20) has already been removed by a similar change of scale of all variables q_i, p_i.

Thus, introducing the more convenient variables $q_1 = x$, $q_2 = y$, $p_1 = p_x$, $p_2 = p_y$, we can rewrite the above Hamiltonian in the form

$$H = \frac{1}{2}(p_x^2 + p_y^2) + V(x, y) = \frac{1}{2}(p_x^2 + p_y^2) + \frac{1}{2}(Ax^2 + By^2) + x^2 y - \frac{C}{3} y^3 = E, \tag{21}$$

where E is the total energy and we have set $\omega_1^2 = A > 0$ and $\omega_2^2 = B > 0$. It is instructive to write down Newton's equations of motion associated with this system

$$\frac{d^2x}{dt^2} = -\frac{\partial V}{\partial x} = -Ax - 2xy, \quad \frac{d^2y}{dt^2} = -\frac{\partial V}{\partial y} = -By - x^2 + Cy^2. \tag{22}$$

Before going further, let us first write down here all possible fixed points of the system, which are easily found by setting the right hand sides in (22) equal to zero:

$$\text{(i)} \quad (x, y) = (0, 0), \quad \text{(ii)} \quad (x, y) = (0, \sqrt{\frac{B}{C}}) \quad \text{(iii)} \quad (x, y) = (\pm\frac{\sqrt{2BA + CA^2}}{2}, -\frac{A}{2}) \tag{23}$$

(the momentum coordinates corresponding to all these points are, of course, zero). The local (or linear) stability of these equilibria will be discussed later, with reference to some very important special cases of the Hénon-Heiles problem. However, there is one of them whose character can be immediately deduced from the above equations: It is, of course, the origin (i), where all nonlinear terms in (22) do not contribute to the analysis. Thus, infinitesimally close to this point, the equations become identical to those of two uncoupled harmonic oscillator (since $A > 0$, $B > 0$) and therefore the equilibrium at the origin is *elliptic*.

Let us remark that (21) represents a first integral of this system. If we could also find a second one, as in the problem of the two harmonic oscillators, with all the nice mathematical properties required by the LA theorem, the problem would be completely integrable and we would be able to integrate the equations (22) by quadratures and obtain the general solution.

This, however, is a very rare occurrence. In most cases that have been numerically solved to date by many authors, even close to the equilibrium point (i), one finds, besides periodic and

quasiperiodic orbits, a new kind of solution that appears "irregular", "unpredictable", one may even say random-looking [20]! These are the orbits called chaotic. They tend to occupy densely 3-dimensional regions in the 4-dimensional phase space and depend very sensitively on initial conditions, in the sense that starting at almost any other point in their immediate vicinity produces another trajectory (also chaotic), which deviates exponentially from the original (reference) orbit as time increases.

Still, if one works only numerically, it is possible to miss chaotic orbits altogether, since their associated regions can be very thin and may not even appear in the computations. To speak about complete integrability therefore (or the absence thereof) one must have some analytical theory to support rigorously one's statements. One such theory is provided by the so-called *Painlevè analysis*, which investigates a very fundamental property of the solutions related to their *singularities in complex time* [9], [16], [28].

The main result here is that if a system of ODEs has the so-called *Painlevè property*, i.e. its solutions have *only poles* as *movable* singularities, it is expected to be completely integrable, even explicitly solvable in terms of known functions. The term "movable" implies that the location of a singularity t_* is one of the free constants to be specified by the initial conditions of the problem. It serves to differentiate movable singularities from the so-called *fixed* ones, which appear explicitly in the equations of motion [11], [18].

In the context of this analysis, one finds that the only known cases in which you can in principle integrate the Hénon-Heiles equations completely are the following:

$$\begin{aligned} \text{Case } 1: &\quad A = B, \quad C = -1, \\ \text{Case } 2: &\quad A, B \text{ free}, \quad C = -6, \\ \text{Case } 3: &\quad B = 16A, \quad C = -16. \end{aligned} \tag{24}$$

Of course, identifying integrable cases by the Painlevè analysis only tells us where to look for N dof Hamiltonian systems whose solutions are globally ordered and predictable. It does not tell us how to find the N integrals that must exist (according to the LA theorem) and which are necessary to solve the equations of motion by quadratures. So, do we really need to bother with examples of integrable systems?

After all, they are so rare, that they can hardly be expected to come up in realistic physical situations. To be fair about them, however, it is important to note that integrable systems are especially useful for two important reasons: First, they frequently arise as close approximations of many physically realistic problems (the solar system being the most famous example) and second, their basic dynamical features do *not* change very much under small perturbations, as the KAM theorem [3] assures us and as we know by now from an abundance of examples.

Let's take for instance the best-studied case of the Hénon-Heiles system, which is both physically interesting and (most likely) non-integrable, $A = B = 1$, $C = 1$ [17], [20]

$$H = \frac{1}{2}(p_x^2 + p_y^2) + \frac{1}{2}(x^2 + y^2) + x^2 y - \frac{1}{3}y^3 = E. \tag{25}$$

Let us select a value of the total energy small enough, within the interval $0 < E < 1/6$, for which it is known that all solutions of (25) are bounded. To visualize these solutions, let us plot in Fig. 7 the intersections of the corresponding orbits with the plane (y, p_y) every time $t = t_k$, $k = 1, 2, \ldots$ at which $x(t_k) = 0$, $p_x(t_k) > 0$. This is what we call a *Poincaré surface of section* (PSS) for which we shall have a lot more to say in the remainder of this section.

Do you see any chaos in panel (a) of this figure, where $E = 1/24$? No. Yet, it is *there*, between the invariant curves that correspond to intersections of 2-dimensional tori of quasiperiodic orbits, in the form of thin chaotic layers that are too small to be visible. To see these chaotic solutions, one would have to either increase the resolution of Fig. 7(a) or raise the energy. Let us do the latter. Observe in this way, in Figs. 7(b), (c), that we would have to reach energy values as high as $E = 1/8$ before we begin to see widespread chaotic regions on the PSS. Note also that these regions grow rapidly as E approaches the escape energy $E = 1/6$, where chaos seems to spread

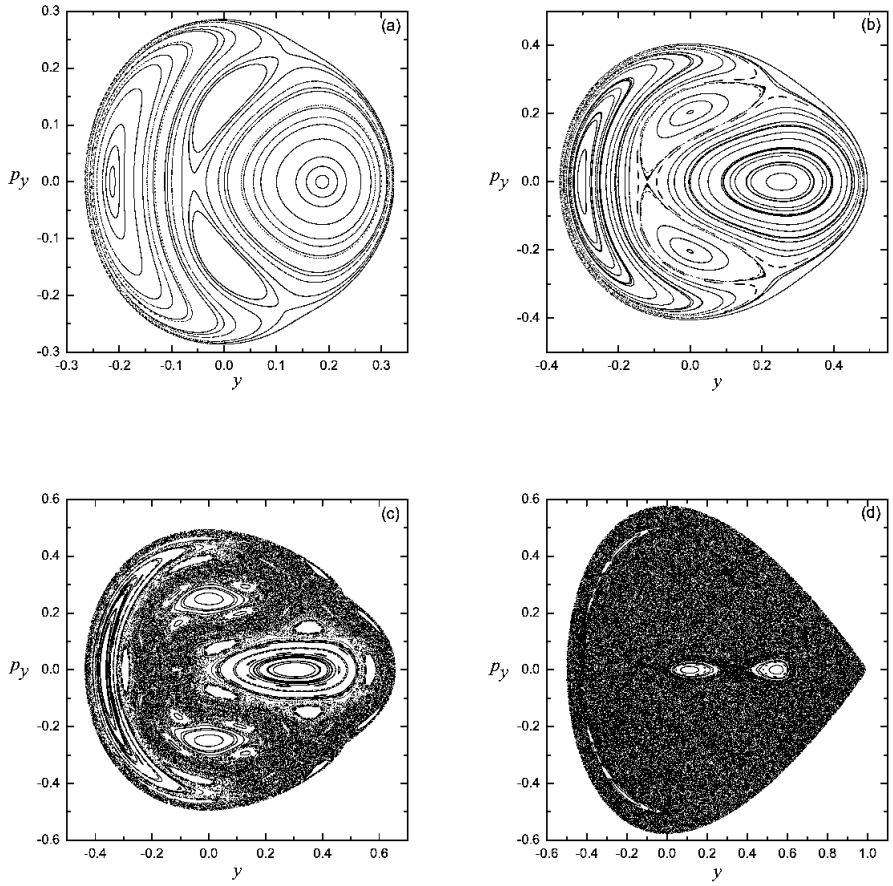

Fig. 7. Orbit intersections with the PSS (y, p_y) of the solutions of the Hénon-Heiles system with Hamiltonian (25), at times t_k, $k = 1, 2, \ldots$, where $x(t_k) = 0$, $p_x(t_k) > 0$ and for fixed values of the energy E. Note in panels (a) and (b), where $E = 1/24$ and $E = 1/12$ respectively, no chaotic orbits are visible and a second integral of motion besides (25) appears to exist. When we raise the energy however to $E = 1/8$ in (c), this is clearly seen to be an illusion. Ordered (i.e. quasiperiodic) motion is restricted within islands surrounded by chaos, whose size diminishes rapidly as the energy increases further. Thus, in (d) where E attains the value $E = 1/6$ above which orbits escape to infinity, the domain of chaotic motion extends over most of the available energy surface.

over the full domain of allowed motion, while regular orbits are restricted within small "islands" of quasiperiodic motion that seem to vanish as the energy increases.

One of the open problems in Hamiltonian dynamics examines the relation between local (linear) stability properties of simple periodic solutions of Hamiltonian systems, and the more "global" dynamics. The general form of the Hamiltonian function that I will be studying in this thesis is given by

$$\begin{aligned} H = \frac{1}{2}\sum_{j=1}^{N} m_j \dot{x}_j^2 + \frac{k}{2}\sum_{j=1}^{N}(x_{j+1} - x_j)^2 + \\ + \frac{\lambda}{1+q}\sum_{j=1}^{N}|x_{j+1} - x_j|^{q+1} = E. \end{aligned} \tag{26}$$

Earlier work by Ch. Antonopoulos and T. Bountis [1] examines this question using a one-dimensional lattice (or chain) of coupled oscillators called the Fermi-Pasta-Ulam β-model (FPU)

described by the N dof Hamiltonian

$$H = \frac{1}{2}\sum_{j=1}^{N} p_j^2 + \sum_{j=1}^{N} \frac{1}{2}(x_{j+1} - x_j)^2 + \\ + \frac{\beta}{4}\sum_{j=1}^{N}(x_{j+1} - x_j)^4 = E, \tag{27}$$

where x_j are the displacements of the particles from their equilibrium positions and $p_j = \frac{dx_j}{dt}$ are the momenta, β is a positive real constant and E is the total energy.

They observed that the FPU system possesses some examples of SPOs, which have well-defined symmetries and are known in closed form, for example:

- the out of phase (pi-mode)

$$\hat{x}_j(t) = -\hat{x}_{j+1}(t) = \hat{x}(t), j = 1, 2, ..., N, \tag{28}$$

  where N is even, under periodic boundary conditions;
- the SPO1 mode, where every 2 particles - one is stationary and those on its either side move out of phase;
- the SPO2 mode, where every 3 particles - one is stationary and the two on either side move out of phase both under fixed boundary conditions.

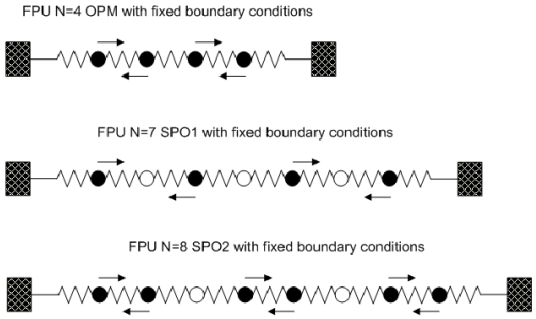

Fig. 8. Examples of SPOs that we have called the Out of Phase (or pi-) Mode (above), the SPO1 (middle) and the SPO2 (below).

Applying Lyapunov's Theorem, one can prove the existence of SPOs for the FPU as continuations of the linear normal modes of the system, whose energies and frequencies are given by [1], [2]

$$E_q = \frac{1}{2}(P_j^2 + \omega_q^2 Q_q^2), \\ \omega_q = 2\sin(\frac{\pi q}{2(N+1)}), q = 1, 2, ..., N, \tag{29}$$

where P_q, Q_q are the normal mode coordinates [20], [26]. SPO1 and SPO2 orbits, for example, can be viewed as nonlinear normal modes identified by indices the $q = \frac{N+1}{2}$ and $q = \frac{2(N+1)}{3}$, respectively in the above equations (29).

In their studies, Bountis and collaborators [1], [2], [5] studied the stability of the above SPOs under small perturbations, as the total energy of the problem E and the number of particles N are increased.They discovered that for small energies these orbits were stable, and there was no chaos around them as they were surrounded by "ellipses" as in Fig. 2 above. However, as E increased there was always some value of $E = E_c(N)$ at which these solutions destabilized and were surrounded by chaos. These authors made two important observations:
1) As the energy increased further, i.e. $E > E_c(N)$ the chaotic regions around SPOs also increased leading from thin layers of "weak chaos" to large regions of "strong" chaos.

2) As the value of N increases indefinitely, it was found that $E_c(N) \to 0$ as $E_c(N) \approx 1/N^a$, where $a = 1$ or $a = 2$.
Thus the main problems of the present thesis are to:

- Study the dynamics of a Hamiltonian Lattice of N nonlinear oscillators, which are used in the analysis of problems of nonlinear elasticity said to be of the Hollomon type [19], [24], [33]
- Write out the nonlinear equations of motion and prove the existence of SPO1, SPO2, or OPM solutions under fixed or periodic boundary conditions.
- Study the stability of these periodic solutions by integrating the system of equations of motion and checking whether neighbouring orbits stay nearby, or move away from the SPO as time grows.
- Evaluate the $E = E_c(N)$ at which these solutions first become unstable and are surrounded by chaos and determine, as the value of N increases, whether $E_c(N) \to 0$ as $E_c(N) \approx 1/N^a$, where $a = 1$ or $a = 2$, like in the FPU system.

Further, we will consider in detail the special case of (26). We will carry out the stability analysis to determine the critical energies $E_c(N)$ where the SPOs first become unstable and try to differentiate between regimes of "weak" chaos and "strong" chaos as the total energy of the system is increased. Stability analysis of these SPO orbits is expected to be different than in FPU nonlinear lattices. Based on our observations, we will try to identify the dynamical properties of oscillators coupled by the Hollomon type of elasticity in engineering. To study the different kinds of chaos that may arise in our problem, we will use the classical tools of Lyapunov exponents measuring the rate of divergence of nearby trajectories in phase space [2], [5], [32].

II. Periodic solutions of Hamiltonian lattices and their stability

A. Equilibrium points, periodic orbits and local stability

Let us note first that Hamilton's equations of motion (1) can be written more compactly in the form

$$\dot{\vec{x}} = \frac{\partial \vec{x}}{\partial t} = \begin{pmatrix} 0_N & I_N \\ -I_N & 0_N \end{pmatrix} \nabla H(\vec{x}) = \Omega \nabla H(\vec{x}), \quad \vec{x} = (\vec{q}, \vec{p}), \tag{30}$$

where I_N and 0_N denote the $N \times N$ identity and zero matrices respectively. This notation, in fact, introduces the important matrix Ω, which is fundamental in establishing the *symplectic structure* of Hamiltonian dynamics. First of all, it enjoys a number of important properties:

$$\text{(i) } \Omega^{\mathrm{T}} = -\Omega \text{ (antisymmetry)}, \ \text{(ii) } \Omega^{\mathrm{T}} = \Omega^{-1} \text{ (orthogonality)}, \tag{31}$$

based on which one defines the *group of symplectic $n \times n$ matrices* M as those that satisfy the condition

$$M = M\Omega M^{\mathrm{T}} \quad \Rightarrow \quad M^{\mathrm{T}} = -\Omega M^{-1} \Omega, \quad M^{-1} = \Omega M^{\mathrm{T}} \Omega^{\mathrm{T}}, \tag{32}$$

with superscripts T and -1 denoting the transpose and inverse of a matrix respectively.

As we discussed in Sect. I, the simplest solutions of a Hamiltonian system are its equilibrium (or fixed points) $(\bar{\vec{q}}, \bar{\vec{p}})$, at which the right hand sides of Hamilton's equations vanish,

$$\frac{\partial H(\bar{\vec{q}}, \bar{\vec{p}})}{\partial \vec{p}_k} = 0, \ \ \frac{\partial H(\bar{\vec{q}}, \bar{\vec{p}})}{\partial q_k} = 0, \ k = 1, 2, \ldots N \tag{33}$$

Thus, given a Hamiltonian system our first task is to find all its fixed points solving the nonlinear equations (33). Next, we need to examine the dynamics near each one of these points.

To do this we write the solutions of (30) as small deviations about one of the fixed points as

$$\vec{x}(t) = (\bar{\vec{q}}, \bar{\vec{p}}) + \vec{\xi}(t), \quad ||\vec{\xi}(t)|| \ll \varepsilon, \tag{34}$$

(where ε is the maximum of the Euclidean norms $||\bar{\vec{q}}||, ||\bar{\vec{p}}||$), substitute in (30) and linearize Hamilton's equations about this point to obtain

$$\dot{\vec{\xi}}(t) = A(\bar{\vec{q}}, \bar{\vec{p}}) \vec{\xi}(t), \tag{35}$$

where higher order terms in $\vec{\xi}$ have been omitted due to the smallness of the norm of $\vec{\xi}(t)$ noted in (34). The constant matrix A represents the Jacobian of $\Omega \nabla H(\vec{x})$ evaluated at the fixed point. The important observation here is that A can be written as the product $A = \Omega S$, where $S = S^{\mathrm{T}}$ is a symmetric matrix.

Clearly, the solutions of the linear system (35) will determine the local stability character of $(\bar{\vec{q}}, \bar{\vec{p}})$ by telling us what kind of dynamics occurs in the vicinity of this equilibrium point. As explained in Sect. I, we shall call this fixed point *linearly stable* if all the solutions of (35) are bounded for all t. To find out under what conditions this is true, let us write the general solution of this system as

$$\vec{\xi}(t) = \exp^{At} \vec{\xi}(0) = X(t) \vec{\xi}(0), \tag{36}$$

where $X(t)$ is called the *fundamental matrix* of solutions of (35), with $X(0) = I_{2N}$, the identity matrix. Clearly, the boundedness properties of these solutions depend on the eigenvalues of the Hamiltonian matrix A. What do we know about these eigenvalues? Many things, it turns out.

Observe that starting from the characteristic equation they satisfy $\det(A - \mu I) = 0$ and using the properties of symmetric matrices and Ω

$$\begin{aligned} \det(A - \mu I) = \det(\Omega S - \mu I) = \det(\Omega S - \mu I)^{\mathrm{T}} = \det(S^{\mathrm{T}} \Omega^{\mathrm{T}} - \mu I) = \\ \det(-S\Omega - \mu I) = (-1)^{2N} \det(S\Omega + \mu I) = \det[\Omega(S\Omega + \mu I)\Omega^{-1}] = \\ \det(\Omega S + \mu I) = \det(A + \mu I) = 0, \end{aligned} \tag{37}$$

we discover that if μ is an eigenvalue of A so is $-\mu$. This implies that Hamiltonian systems can never have asymptotically stable (or unstable) fixed points. We, therefore, conclude that a necessary

and sufficient condition for such a equilibrium point to be stable is that all the eigenvalues of its corresponding matrix A have zero real part! And since A is a real matrix, if it possesses an eigenvalue $\mu = \alpha + i\beta$ (with α, β real), it will also have among its eigenvalues: $\mu = \alpha - i\beta$, $\mu = -\alpha + i\beta$ $\mu = -\alpha - i\beta$.

Now we understand why in all the $N = 1$, $N = 2$ dof Hamiltonian systems studied in Sect. I, all stable fixed points have A matrices with purely imaginary eigenvalues and the solutions in their neighborhood execute simple harmonic motion. Furthermore, we also realize that a stable fixed point of a Hamiltonian system can become unstable by two kinds of *bifurcations*:

(i) A pair of imaginary $(\pm i\beta)$ eigenvalues splitting *on the real axis* into an $(\alpha, -\alpha)$ pair, or

(ii) An eigenvalue pair $(\pm i\beta)$ splitting into four eigenvalues $(\pm\alpha \pm i\beta)$ in the complex plane, in a type of *complex instability*.

Bifurcation (i) leads to an equilibrium of the *saddle* type, since $(\alpha, -\alpha)$ correspond to two real eigenvectors, along which the solutions of (35) converge or diverge exponentially from the fixed point. These eigenvectors identify the so-called stable and unstable *euclidean* manifolds, respectively, E^s, E^u, of the fixed point. When continued under the action of the full nonlinear equations of motion (30) these become the stable and unstable invariant manifolds W^s, W^u, which may intersect each other (or invariant manifolds of other saddle fixed points) and cause the horseshoe type of homoclinic (or heteroclinic) chaos we already encountered in the examples of Sect. I.

By contrast, bifurcation (ii) occurs more rarely because it requires that the four imaginary eigenvalues of a stable equilibrium point, $(\pm i\beta_1, \pm\beta_2)$, be *degenerate*, i.e. $\beta_1 = \beta_2$. It also does not arise in Hamiltonian systems of $N = 1$ dof.

It is time now to discuss the next most important type of solution of Hamiltonian systems, which is their periodic orbits. You might expect, of course, the mathematics here to become more involved and you would be right. However, as we will soon find out, the wonderful instrument of the Poincaré map and its associated surfaces of section will come to the rescue and make the analysis a lot easier. Let us begin by giving a more general definition of the Poincaré map than the one we used in Sect. I.

In particular, we will assume that our n-dimensional dynamical system, cast in the general form $\dot{\vec{x}} = \vec{f}(\vec{x})$ has a periodic solution $\hat{\vec{x}}(t) = \hat{\vec{x}}(t + T)$ of period T. Let us choose an arbitrary point along this orbit $\hat{\vec{x}}(t_0)$ and define a PSS at that point as follows

$$\Sigma_{t_0} = \left\{ \vec{x}(t) \;\; / \;\; (\vec{x}(t) - \hat{\vec{x}}(t_0)) \cdot \vec{f}(\hat{\vec{x}}(t_0)) = 0 \right\}. \tag{38}$$

Thus, Σ_{t_0} is a $(n-1)$-dimensional plane which intersects the given periodic orbit at $\hat{\vec{x}}(t_0)$ and is vertical to the direction of the flow at that point. Clearly now a Poincaré map can be defined on that plane as before, by

$$P : \Sigma_{t_0} \to \Sigma_{t_0}, \quad \vec{x}_{k+1} = P\vec{x}_k, \quad k = 0, 1, 2, \ldots \tag{39}$$

for which $\vec{x}_0 = \hat{\vec{x}}(t_0)$ is a fixed point, since $\vec{x}_0 = P\vec{x}_0$. We now examine small deviations about this point,

$$\vec{x}_k = \hat{\vec{x}}_0 + \vec{\eta}_k, \quad ||\vec{\eta}_k|| \ll \varepsilon, \tag{40}$$

(where ε is of the same magnitude as $||\hat{\vec{x}}_0||$), substitute (40) in (39) and linearize the Poincaré map to obtain

$$\vec{\eta}_{k+1} = DP(\hat{\vec{x}}_0)\vec{\eta}_k, \tag{41}$$

where we have neglected higher order terms in $\vec{\eta}$ and $DP(\hat{\vec{x}}_0)$ denotes the Jacobian of P evaluated at $\hat{\vec{x}}_0$.

To determine P we may use the *variational equations* of the original differential equations derived by writing $\vec{x}(t) = \hat{\vec{x}}(t) + \vec{\xi}(t)$, whence linearizing original dynamical system of first order ODEs about this periodic orbit leads to the system

$$\dot{\vec{\xi}}(t) = A(t)\vec{\xi}(t), \quad A(t) = A(t + T), \tag{42}$$

where $A(t)$ is the Jacobian matrix of $\vec{f}(\vec{x})$ evaluated at the periodic orbit $\vec{x}(t) = \hat{\vec{x}}$. The crucial question, of course, we must face now is: How are the two linear systems (41) and (42) related to each other?

Observe that we have used different notations for the small deviations about the periodic orbit: $\vec{\xi}(t)$ in the continuous time setting of differential equations and $\vec{\eta}_k$ in the discrete time setting of the Poincaré map. This is not just because they represent different quantities, it is also to emphasize that their dimensionality as vectors in the n-dimensional phase space $\mathbb{R}^n$ ($n = 2N$ for a Hamiltonian system) is different: $\vec{\xi}(t)$ is n-dimensional, while $\vec{\eta}_k$ is $(n-1)$-dimensional! How are we to match these two small deviation variables?

The answer will come from what is called *Floquet theory* [11], [27], [34]. First we realize that since (42) is a linear system of ODEs it must possess, in general, n linearly independent solutions, forming the columns of the $n \times n$ *fundamental solution* matrix $M(t, t_0)$ in

$$\vec{\xi}(t) = M(t, t_0)\vec{\xi}(0), \quad M(t, t_0) = M(t + T, t_0) \tag{43}$$

(see (36)). Now, if we change our basis at the point $\hat{\vec{x}}(t_0)$ so that one of the directions of motion is along the direction *vertical* to the PSS (38), we will observe that the nth column of the matrix $M(T, t_0)$ has zero elements except at the last entry which is 1. Thus, if we eliminate from this matrix its nth row and nth column, it turns out that its $(n-1) \times (n-1)$ submatrix is none other than our beloved Poincaré map (39)! Surprised? That is the relation between the two approaches we were seeking.

This means that if we could compute the so-called monodromy matrix $M(T, t_0)$ numerically we could evaluate its eigenvalues, $\mu_1, \ldots, \mu_{n-1}$ (the last one being $\mu_n = 1$), which are those of the Poincaré map and determine the stability of our periodic orbit as follows: If they are all on the unit circle, i.e. $|\mu_i| = 1, \quad i = 1, \ldots, n-1$, the periodic orbit is (linearly) *stable*, while if (at least) one of them satisfies $|\mu_j| > 1$ the periodic solution is *unstable* .

But how do we compute the monodromy matrix $M(T, t_0)$? It is not so difficult. Let us first set $t_0 = 0$ for convenience and observe from (43) that $M(0, 0) = I_n$. All we have to do is integrate numerically the variational equations (43) from $t = 0$ to $t = T$, n times, each time for a *different* initial vector $(0, \ldots, 0, 1, 0, \ldots, 0)$ with 1 placed in the ith position, $i = 1, 2, \ldots, n$. Note that since these equations are linear numerical integration can be performed to *arbitrary accuracy* and is also not too-time consuming for reasonable values of the period T. Once we have calculated $M(T, 0)$, we may proceed to compute its eigenvalues and determine the stability of the periodic orbit according to whether at least one of these eigenvalues has magnitude greater than 1.

B. Implications about global stability as $N \to \infty$

Now that we have learned how to study the linear stability properties of periodic solutions of Hamiltonian systems, it is time to wonder about the implications of this analysis regarding the more "global" dynamics, which is really what we are interested in. Let us turn, therefore, immediately to the class of one-dimensional lattices (or chains) of coupled oscillators.

Our first example is the famous Fermi Pasta Ulam (FPU)$-\beta$ model described by the N dof Hamiltonian [4]

$$H = \frac{1}{2}\sum_{j=1}^{N} p_j^2 + \sum_{j=0}^{N} \frac{1}{2}(x_{j+1} - x_j)^2 + \frac{1}{4}\beta(x_{j+1} - x_j)^4 = E, \tag{44}$$

where x_j are the displacements of the particles from their equilibrium positions, and $p_j = \dot{x}_j$ are the corresponding canonically conjugate momenta, β is a positive real constant and E is the total energy of the system. Note that by not including any cubic nearest neighbor interactions in (44), we have kept an important symmetry of the system under the interchange $x_j \to -x_j$, which will make our analysis simpler. However, most of what we shall be discussing can also be studied when cubic interactions are included with an α coefficient before them in what is called the FPU-α model.

Let us focus on the special class of periodic solutions we have called Simple Periodic Orbits (SPOs), which have well-defined symmetries and are known in closed form. In particular the SPOs we shall be concerned with are the following:
I. For the FPU with *periodic boundary conditions*:

$$x_{N+k}(t) = x_k(t), \ \forall t, k \tag{45}$$

The Out-of-Phase Mode (OPM) for FPU, with N even (often called the π-mode)

$$\hat{x}_j(t) = -\hat{x}_{j+1}(t) \equiv \hat{x}(t), \quad j = 1, \ldots, N. \tag{46}$$

II. For the FPU model and *fixed boundary conditions*:

$$x_0(t) = x_{N+1}(t) = 0, \ \forall t \tag{47}$$

(a) The SPO1 mode, with N odd,

$$\hat{x}_{2j}(t) = 0, \quad \hat{x}_{2j-1}(t) = -\hat{x}_{2j+1}(t) \equiv \hat{x}(t), \quad j = 1, \ldots, \frac{N-1}{2}. \tag{48}$$

(b) The SPO2 mode, with $N = 5 + 3m, \ m = 0, 1, 2, \ldots$ particles,

$$\begin{aligned} x_{3j}(t) &= 0, \quad j = 1, 2, 3 \ldots, \frac{N-2}{3}, \\ x_j(t) &= -x_{j+1}(t) = \hat{x}(t), \quad j = 1, 4, 7, \ldots, N-1. \end{aligned} \tag{49}$$

Fortunately, the FPU system with fixed boundary conditions is one of those examples where we can directly apply Lyapunov's Theorem. More specifically, we can use it to *prove the existence* of SPOs as continuations of the linear normal modes of the system, whose frequencies have the well-known form [4], [8], [14], [15], [20]

$$\omega_q = 2 \sin \left(\frac{\pi q}{2(N+1)} \right), \quad q = 1, 2, \ldots, N. \tag{50}$$

This is so because the linear mode frequencies (50) are seen to satisfy Lyapunov's non-resonance condition for the ω_qs, stated in Lyapunov's Theorem for all q and general values of N. Thus, our SPO1 and SPO2 orbits, as NNMs of the FPU Hamiltonian, are identified by the indices $q = (N+1)/2$ and $q = 2(N+1)/3$ respectively.

As we discussed in the previous section, linear stability analysis of periodic solutions can be performed by studying the eigenvalues of the monodromy matrix. This leads to the interesting result that the critical energy threshold values for the first destabilization of the SPO1 solution satisfies $E_c/N \propto 1/N$, while for the OPM solution (46) we find $E_c/N \propto 1/N^2$, as shown in Figs. 9(a) and (b) respectively.

What does all this mean? Let us try to find out.

As we discovered from the above analysis, the NNMs of the FPU Hamiltonian studied so far experience a first destabilization at energy densities of the form

$$\frac{E_c}{N} \propto N^{-\alpha}, \ \alpha = 1, \text{or, } 2, \ \ N \to \infty. \tag{51}$$

This means that for fixed N, some of these fundamental periodic solutions become unstable at much lower energy than others. We may, therefore, expect that those that destabilize at lower energies will have *smaller* chaotic regions around them, as the greater part of the constant energy surface is still occupied by tori of quasiperiodic motion. Could we then perhaps argue that near NNMs characterized by the exponent $\alpha = 2$ in (51) one would find a "weaker" form of chaos than in the $\alpha = 1$ case?

This indeed appears to be true at least for the FPU Hamiltonian model. As was recently shown in [14], the energy threshold for the destabilization of the low $q = 1, 2, 3, \ldots$, nonlinear modes,

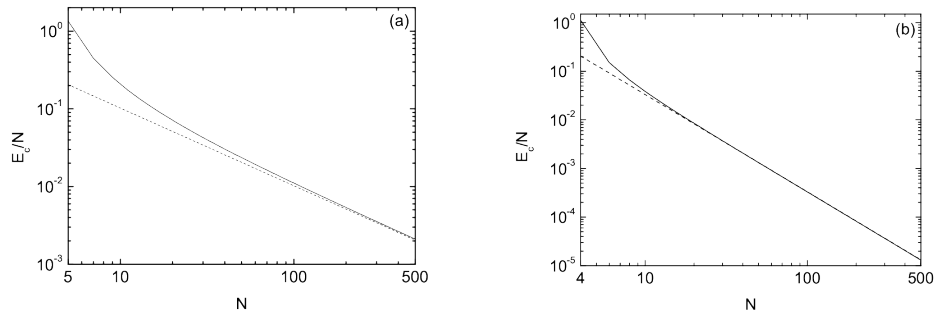

Fig. 9. (a) The solid curve corresponds to the energy per particle E_c/N, for $\beta = 1$, of the first destabilization of the SPO1 nonlinear mode of the FPU system (44) with fixed boundary conditions, obtained by the numerical evaluation of the monodromy matrix, while the dashed line corresponds to the function $\propto 1/N$. (b) Same as in (a) with the solid curve depicting the first destabilization of the OPM periodic solution of the FPU system (44). Here, however, the dashed line corresponds to the function $\propto 1/N^2$, i.e $\alpha = 2$. Note that both axes are logarithmic (after [2]).

representing continuations of the corresponding linear modes (see (50)), satisfies the analytical formula

$$\frac{E_c}{N} \approx \frac{\pi^2}{6\beta N(N+1)}, \tag{52}$$

and is therefore of the type $\alpha = 2$ in (51). Remarkably enough this local loss of stability coincides with the "weak" chaos threshold shown in [12], [13] to have global consequences regarding the dynamics of the system as a whole, as it is associated with the breakup of the famous *FPU recurrences*! For the moment, let us simply point out that the destabilization of individual NNMs occurring at low energies appears to be somehow related to a transition from a "weak" to a "stronger" type of chaos in the full N particle chain.

Interestingly enough, it was later discovered [1], [2] that the energy threshold (52) for the low q modes, also coincides with the instability threshold of our SPO2 mode which corresponds to $q = 2(N+1)/3$! In Fig. 10 we compare the approximate formula (dashed line) with our destabilization threshold for SPO2 obtained by the monodromy matrix analysis (solid line) for $\beta = 0.0315$ and find excellent agreement especially in the large N limit.

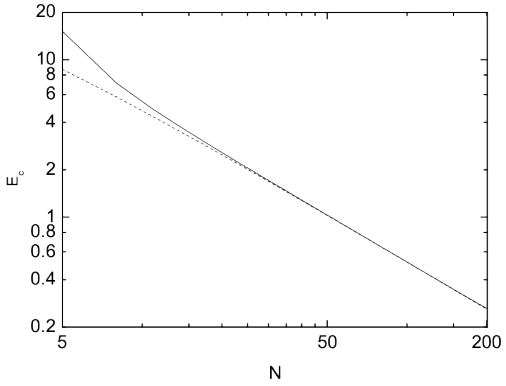

Fig. 10. The solid curve corresponds to the energy $E_{2u}(N)$ of the first destabilization of the SPO2 mode of the FPU system (44) with fixed boundary conditions and $\beta = 0.0315$ obtained by the numerical evaluation of the eigenvalues of the monodromy matrix. The dashed line corresponds to the approximate formula (51) for the $q = 3$ nonlinear normal solution (after [1]) hence SPO2 also has $\alpha = 2$.

We may, therefore, arrive at the following conclusions based on the above results: Linear stability (or instability) of periodic solutions is certainly a local property and can only be expected to reveal how orbits behave in a limited region of phase space. And yet, we find that if these periodic solutions

belong to the class of nonlinear continuations of linear normal modes, their stability character may have important consequences for the global dynamics of the Hamiltonian system. In particular, if the exponent of their first destabilization threshold in (51) is $\alpha = 2$ they are connected with the onset of "weak" chaos as a result of the breakdown of FPU recurrences. On the other hand, if $\alpha = 1$ as in the case of the SPO1 mode, they arise in much wider chaotic domains and have orbits in their neighborhood which evolve from "weak" to "strong" chaos passing through quasi-periodic states of varying complexity, with different *statistical* properties.

III. Application to a lattice of Hollomon oscillators

A. A Single Hollomon Oscillator

Let us now turn to study an application of the above results on another 1–Dimensional Hamiltonian lattice of nonlinear oscillators that are very different from the FPU lattice of the previous chapter. Each oscillator of this lattice obeys the second order ODE:

$$H = \frac{m}{2}\dot{x}^2 + \frac{k}{2}x^2 + \frac{\lambda}{1+q}|x|^{1+q}. \tag{53}$$

which has been used in the analysis of problems of nonlinear elasticity of the Hollomon type [7], [19], [24], [29], [33], describing what is known in engineering as "work hardening". The exponent q captures the relevant fractional nonlinearities in such models. For $q = 1$ the former equation recovers the Hamiltonian of a harmonic oscillator with the oscillation constant $k' = k + \lambda$. For $q = 3$ it describes the Hamiltonian of the Fermi-Pasta-Ulam model for a single oscillator. From the Hamiltonian (53) we determine the equation of motion of the single oscillator as

$$m\ddot{x} + kx + \lambda|x|^{q-1}x = 0\,, \tag{54}$$

This ODE cannot be solved in a closed form with respect to $x(t)$. Moreover, it is of central importance to our analysis since the special SPO1 and SPO2 solutions we will study below collapse to the ODE (54) obeyed by all moving particles. Furthermore, since it is derived from a positive definite potential with a single minimum at $x = 0$, it is clear that its solutions are periodic with a frequency ω that depends on the initial conditions.

Thus, we proceed to solve (54) expanding $x(t)$ in a Fourier series up to order n, where the higher the value of n the better the approximation of the series.

$$x_n(t) = \sum_{i=1}^{n} A_i \cos(i\omega_n t)\,, \tag{55}$$

where $x(t) = \lim_{n\to\infty} x_n(t)$. Accordingly, we need to determine the coefficients A_i and the oscillation frequency ω_n, which is the $n-th$ order approximation to the actual frequency ω. Our solution scheme presented below is such that the oscillation energy E is always preserved.

Multiplying Eq. (54) with x we obtain $\lambda|x|^{q+1} = -mx\ddot{x} - kx^2$. Substituting the q-dependent term of this equation into Eq. (53) and equating the Hamiltonian with the value of the constant energy E of the oscillator we write the latter as

$$E = \frac{m}{2}\dot{x}^2 + C_1\,x^2 + C_2\,x\ddot{x}\,, \qquad C_1 \equiv \frac{k(q-1)}{2(q+1)}\,, \qquad C_2 \equiv -\frac{m}{q+1}\,. \tag{56}$$

By virtue of Eq. (55) the energy can be expressed as a series of trigonometric functions,

$$\begin{aligned} E &= \frac{m\omega_n^2}{2}[\sum_{i=1}^{n} iA_i \sin(i\omega_n t)]^2 + C_1[\sum_{i=1}^{n} A_i \cos(i\omega_n t)]^2 \\ &\quad - C_2\,\omega_n^2[\sum_{i=1}^{n} A_i \cos(i\omega_n t)][\sum_{j=1}^{n} j^2 A_j \cos(j\omega_n t)]\,. \end{aligned} \tag{57}$$

Using standard trigonometric identities turning products of trigonometric functions into single sines and cosines we rewrite each term on the rhs of Eq. (57) as

$$\begin{aligned} [\sum_{i=1}^{n} iA_i \sin(i\omega_n t)]^2 &= \sum_{i=1}^{n}\sum_{j=1}^{n}(iA_i)(jA_j)\sin(i\omega_n t)\sin(j\omega_n t) \\ &= \frac{1}{2}\sum_{i=1}^{n}\sum_{j=1}^{n}(iA_i)(jA_j)\Big\{\cos[(i-j)\omega_n t] - \cos[(i+j)\omega_n t]\Big\}\,, \end{aligned} \tag{58}$$

$$[\sum_{i=1}^{n} A_i \cos(i\omega_n t)]^2 = \sum_{i=1}^{n}\sum_{j=1}^{n} A_i A_j \cos(i\omega_n t)\cos(j\omega_n t)$$
$$= \frac{1}{2}\sum_{i=1}^{n}\sum_{j=1}^{n} A_i A_j \Big\{ \cos[(i-j)\omega_n t] + \cos[(i+j)\omega_n t]\Big\}, \quad (59)$$

and

$$[\sum_{i=1}^{n} A_i \cos(i\omega_n t)][\sum_{j=1}^{n} j^2 A_j \cos(j\omega_n t)] = \sum_{i=1}^{n}\sum_{j=1}^{n} j^2 A_i A_j \cos(i\omega_n t)\cos(j\omega_n t)$$
$$= \frac{1}{2}\sum_{i=1}^{n}\sum_{j=1}^{n} j^2 A_i A_j \Big\{ \cos[(i-j)\omega_n t] + \cos[(i+j)\omega_n t]\Big\}$$

so that finally Eq. (57) takes the form

$$E = \sum_{i=1}^{n}\sum_{j=1}^{n} a_{i,j}^{(+)} \cos[(i-j)\omega_n t] + \sum_{i=1}^{n}\sum_{j=1}^{n} a_{i,j}^{(-)} \cos[(i+j)\omega_n t] \quad (60)$$

with

$$a_{i,j}^{(\pm)} := \frac{1}{2}\Big(C_1 - C_2\,\omega_n^2\, j^2 \pm \frac{m\omega_n^2}{2} ij\Big) A_i A_j\,. \quad (61)$$

Expressing the initial condition of the equation as $x(0) = x_0 = \sum_{i=1}^{n} A_i$ and setting with no loss of generality $\dot{x}(0) = 0$, we derive from Eq. (60) an analytical expression of the oscillation frequency in terms of the Fourier A_i coefficients,

$$\omega_n^2 = \frac{C_1 x_0^2 - E}{C_2\, x_0 \sum_{j=1}^{n} j^2 A_j}\,. \quad (62)$$

Now, we equate to zero all terms in (60) proportional to the different cosine modes, since they are linearly independent, and obtain $n-1$ equations to determine the $A_1, \ldots, A_n$ coefficients. The missing nth equation is given by the initial condition (62) above. Thus, we find

$$E = \sum_{i=1}^{n-1} Q_i^{(n)} \cos[(i-1)\omega_n t]\,, \qquad Q_i^{(n)} := 2^{-\delta_{i-1,0}} \sum_{j=1}^{n-i+1} \Big(a_{j,j+i-1}^{(+)} + a_{j+i-1,j}^{(+)}\Big) + \sum_{j=1}^{i-2} a_{j,i-1-j}^{(-)}\,, \quad (63)$$

where δ_{ij} is the Kronecker delta function and $n \geq 1$. Indeed, we thus find $Q_1^{(n)} = E$, $Q_2^{(n)} = 0, \ldots, Q_{n-1}^{(n)} = 0$, while the nth equation becomes. $Q_n^{(n)} := \sum_{i=1}^{n} A_i - x_0 = 0$. After having determined the coefficients $\{A_j\}_{j=1}^{n}$, we substitute them back into Eq. (62) and calculate the oscillation frequency ω_n. Clearly, we expect that the more terms we consider the better the convergence to $\omega = \lim_{n\to\infty} \omega_n$ will be.

To demonstrate graphically the convergence of our approximations to the correct periodic solution of the problem, we set $k = 0.1$, $\lambda = 1.05$, $m = 1$ and $E = 1$ and evaluate the corresponding results analytically and numerically. In Table III-A we have recorded for $q = 1/3$ and for various n's the coefficients $\{A_i\}_{i=1,\ldots,n}$ determined from the preceding system of equations, i.e. $\{Q_i^{(n)}\}_{i=1,\ldots,n} = 0$.

In Fig. 11a) we plot the numerical solution of Eq. (54) within a period for the position $x(t)$ (red stars) and the velocity $v(t)$ (blue spheres) with the initial values $x(0) = x_0$ and $v(0) = 0$, and the exponent $q = 1/3$. The amplitude x_0 is calculated for the given values of the parameters from Eq. (53). In Fig. 11b) we zoom at the vicinity of the minimum velocity (black spheres) and plot our approximate analytical solution for $n = 3$ (blue dashed line), $n = 5$ (green dashed-dotted line) and $n = 7$ (red solid line). As can be seen, the higher the number of terms n in the Fourier expansion the better the approximation of the numerical solution, as expected.

TABLE I

THE COEFFICIENTS OF THE FOURIER SERIES EXPANSION FOR VARIOUS n AFTER SOLVING THE SYSTEM OF EQUATIONS $\{Q_i^{(n)}\}_{i=1,\ldots,n} = 0$ FOR $q = 1/3$.

q	n	A_1	A_2	A_3	A_4	A_5	A_6	A_7	ω_n
	3	1.15549	0	−0.0178126	-	-	-	-	1.10262
1/3	5	1.15999	0	−0.0251842	0	0.00286947	-	-	1.09717
	7	1.15905	0	−0.0250019	0	0.00450762	0	−0.000878732	1.09794

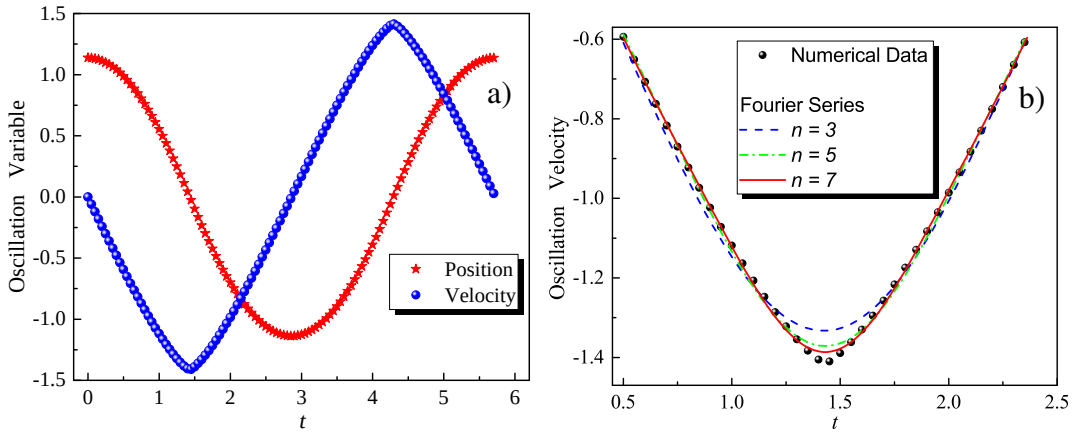

Fig. 11. a) Plot of the numerical solution of the position and velocity functions in Eq. (54) with respect to time for the rational exponent $q = 1/3$, b) Evidence of convergence of the Fourier series expansion for increasing n to the velocity function (black spheres) at the vicinity of its minimum value within a period. As expected, the higher the value of n the better the approximation.

B. Simple Periodic Orbits of the Hollomon Lattice

Let us consider now a 1-Dimensional nonlinear lattice of N nearest-neighbor interacting oscillators of the Hollomon type described by the Hamiltonian

$$H = \frac{1}{2}\sum_{j=1}^{N} m_j \dot{x}_j^2 + \frac{k}{2}\sum_{j=0}^{N}(x_{j+1}-x_j)^2 + \frac{\lambda}{q+1}\sum_{j=0}^{N}|x_{j+1}-x_j|^{q+1}\,, \tag{64}$$

whose $j = 1, \ldots, N$ equations of motion are:

$$m_j\ddot{x}_j \;=\; k(x_{j-1}-2x_j+x_{j+1}) - \lambda\left(|x_j-x_{j-1}|^q\frac{x_j-x_{j-1}}{|x_j-x_{j-1}|} - |x_{j+1}-x_j|^q\frac{x_{j+1}-x_j}{|x_{j+1}-x_j|}\right) \tag{65}$$

under fixed boundary conditions at both ends, see Fig. I-B, and zero initial velocities.

$$x_0(t) = x_{N+1}(t) = \dot{x}_0(t) = \dot{x}_{N+1}(t) = 0\,, \qquad \forall t \geq 0. \tag{66}$$

As before, $H = E$ is the total energy of the system. Introducing the sign function as

$$\mathrm{sgn}(x-x_0) = \frac{x-x_0}{|x-x_0|} = \begin{cases} 1 & ,x > x_0 \\ -1 & ,x < x_0 \end{cases}. \tag{67}$$

we rewrite the system of differential equations (65) in the form

$$m_j\ddot{x}_j \;=\; k(x_{j-1}-2x_j+x_{j+1}) - \lambda\Big[|x_j-x_{j-1}|^q\mathrm{sgn}(x_j-x_{j-1}) - |x_{j+1}-x_j|^q\mathrm{sgn}(x_{j+1}-x_j)\Big].$$

When $q \geq 1$ the discontinuity in the sign function when $\Delta x_j = 0$ does not create difficulties regarding the numerical integration since the term $|\Delta x_j|^q = 0$ dominates. However, when $q \in [0, 1)$, which is of interest in our study, the sign function dominates over the term $|\Delta x_j|^q$ creating fluctuations in the solutions, which are higher the higher the energy. We stress that these fluctuations are not of physical but of numerical nature. Thus, the method we adopt here to avoid this undesired behavior in the numerical integration of Eq. (65) for $q \in [0, 1)$ is to approximate the sign function,

for small displacements $\hat{x}(t) \in [-0.5, 0.5]$, by the smooth function $\tanh(\tau\hat{x}(t))$ for a large value of τ, $\tau > 100$, which determines the steepness of the slope of the function at $\hat{x}(t) = 0$, since higher values of τ correspond to steeper slopes.

In what follows, we will apply the above analysis first to evaluate exactly particular oscillation modes, such as the SPO1 and SPO2 of Fig. I-B, for the Hollomon lattice described by Eqs. (64) and (68) with all masses $m_j = 1$, and $q = 1/3$. Note that for SPO1 there is one stationary particle between each pair of oppositely moving ones, while for SPO2 there two oppositely moving particles between each stationary one. The calculation of these periodic modes is immediate because all particles (except the stationary ones) execute the *same* periodic motion (with alternating phases), as described in (54), whose solution we just obtained in terms of Fourier series.

The interesting question that arises now is how do these solutions behave under small changes in their initial conditions? Do small perturbations of their positions and/or velocities lead to orbits which stay close to the SPO for all time? If that were the case, we call the SPO *stable* and hence free from chaos in its immediate neighborhood. If, on the other hand, small deviations of the SPO lead to entirely different regions of phase space, the SPO is called *unstable* and we expect to find chaos in its vicinity.

Typically, the analysis of the stability properties of an SPO is made by solving the appropriate linear variational equations and using Floquet theory to calculate the eigenvalues of monodromy matrices [1], [2]. However, for $q \in [0, 1)$, these approaches cannot be straightforwardly applied because they rely on taking derivatives of terms containing absolute value terms that are not everywhere differentiable.

We shall, therefore, employ a different, more "practical" approach to study the stability of our SPO solutions. More specifically, we will select small perturbations of the initial conditions of a given SPO and solve numerically Eq. (65) to study the behaviour of the distance function $D(t)$, defined as the euclidean distance between the SPO and its perturbation:

$$D(t) = \sqrt{\sum_{j=1}^{N} [\Big(\hat{x}_{i,p}(t) - \hat{x}_{i,unp}(t)\Big)^2 + \Big(\dot{\hat{x}}_{i,p}(t) - \dot{\hat{x}}_{i,unp}(t)\Big)^2]} \,. \tag{68}$$

where the indices p and unp denote the perturbed and unperturbed solution, respectively. Clearly, if the SPO solution is *stable*, when subjected to small perturbations, it will yield small vaues of $D(t)$, oscillating about zero with a small amplitude which is known to grow *linearly* in time. However, if the SPO is *unstable* $D(t)$ is expected to grow *exponentially*.

1) The case of the SPO1 orbit: $k = 1$, $\lambda = 1.04$

The SPO1 orbit is a particularly simple periodic solution studied in [2], [6], [25], which occurs with an odd number $N = 3 + 2\nu$, $\nu \in \mathbb{N}$ of oscillating sites, and is defined as

$$\hat{x}_{2j}(t) = 0 \,, \quad \hat{x}_{2j-1}(t) = -\hat{x}_{2j+1}(t) \equiv \hat{x}(t) \,, \qquad j = 1, \ldots, \frac{N-1}{2} \tag{69}$$

This means that among the N sites every second site is stationary so that only $N_* = (N+1)/2$ sites oscillate. Using the abbriviations $\hat{k} \equiv 2k$, $\hat{\lambda} \equiv 2\lambda$ and $\hat{E} \equiv E/N_*$, Eq. (68) reduces to a sigle differential equation for $\hat{x}(t)$, namely

$$\ddot{\hat{x}} = -\hat{k}\hat{x} - \hat{\lambda}|\hat{x}|^{q-1}\hat{x} \tag{70}$$

of the energy

$$\hat{E} = \frac{1}{2}\dot{\hat{x}}^2 + \frac{\hat{k}}{2}\hat{x}^2 + \frac{\hat{\lambda}}{q+1}|\hat{x}|^{q+1} \,. \tag{71}$$

As can be seen, the equation of motion and the energy expression of this reduced oscillatory mode is exactly the one we studied in Eqs. (53) and (54). Thus, the solution $\hat{x}(t)$ and the oscillation frequency ω_n are calculated as before by solving the system of $n-1$ nonlinear equations in Eq. (63) and the initial condition for $E \to \hat{E}$, $k \to \hat{k}$ and $\lambda \to \hat{\lambda}$.

To calculate numerically the distance function $D(t)$ between SPO1 and its perturbation, we have introduced small perturbations in the initial values for $t = 0$ as follows

$$\hat{x}_{2j}(0) = \epsilon_{2j} \in [10^{-5}, 10^{-4}]\,. \tag{72}$$

To keep the energy of the system unaltered, we compensate the above changes by introducing a correction term η in the initial condition of the first oscillator, $\hat{x}_1(0) = x_0 - \eta$, determined from Eq. (64).

For very small values of the energy, the distance function in Eq. (68) grows linearly, indicating that the corresponding SPO1 solution is stable. However, as E grows, there is a critical energy $E = E_c$ above which $D(t)$ starts to grow exponentially, suggesting that for $E \geq E_c$ SPO1 has become unstable. We call this E_c the first destabilization energy of the system. Evaluating numerically the corresponding *energy density* $\mathcal{E} \equiv E_c/N$, we plot it in a double logarithmic scale with solid black spheres in Fig. 12, as a function of N.

Remarkably, the results show a very different situation than what we have encountered for the FPU lattice in the previous chapter in Fig. 9 and Fig. 10! Instead of E_c/N decreasing towards zero as one would normally expect, in the Hollomon lattice the opposite is true: The system appears to become more and more stable as it's size grows for higher and higher N.

Instead of following a decaying power law as described in Eq. (51), the E_c/N curve for the Hollomon lattice, as shown by the red line in Fig.12, is well–fitted by a function of the form $\mathcal{E}(N) = a + bN^c$ given explicitly by the expression

$$\mathcal{E}(N) = 0.6 + 0.02\ N^{2.82}\,. \tag{73}$$

Thus, we conclude that for large values of N the density $\mathcal{E}$ exhibits a power law behaviour with a positive exponent. This is a new and unexpected result, which can only be due to the properties of elastic materials described by Hollomon's law. It implies that the lattice as a whole may be insensitive to small perturbations and maintain its stability even for large values of E and N. This is quite the opposite than has been observed in all other lattices to date, where the limit of $E \to \infty$ and $N \to \infty$ with $E/N = const.$ is associated with instabilities for almost any finite energy value [1], [2].

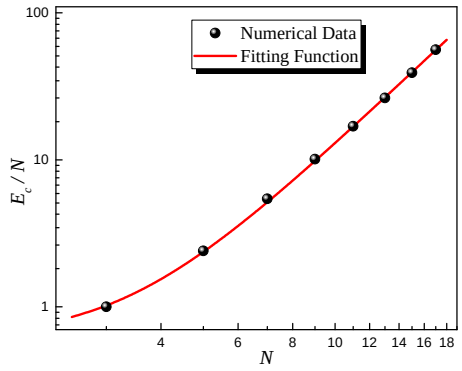

Fig. 12. Critical energy density graph for the SPO1 solution in a double logarithmic scale.

Of course, the above conclusions are drawn from studying the stability properties of only one SPO. As we have stressed in previous chapters, SPOs are very important as they constitute

continuations of linear normal modes of lattices into the nonlinear regime. However, further study is needed concerning analogous properties of other SPOs before general statements can be made about Hollomon lattices.

2) The case of the SPO-2 orbit: $k = 1$, $\lambda = 1.04$

In order to draw more general conclusions, therefore, we have decided to perform the same analysis for the SPO2 orbit, where there are two particles between each stationary one, moving opposite to each other. Under fixed boundary conditions, SPO2 solutions occur with $N = 3{+}2n$, $n \in \mathbb{N}$ oscillating sites, defined by

$$x_{3j}(t) = 0\,, \qquad j = 1, 2, 3, \ldots, \frac{N-2}{3} \tag{74}$$

$$x_j(t) = -x_{j+1}(t) \equiv \hat{x}(t)\,, \qquad j = 1, 4, 7, \ldots, N-1 \tag{75}$$

This means that among the N sites only $N_* = 2(N+1)/3$ oscillate. Using here the substitutions $\hat{k} \equiv 3k$, $\hat{\lambda} \equiv \lambda(1+2^q)$ and $\hat{E} \equiv E/N_*$ we can compute exactly SPO2 orbits by solving the single oscillator equation described by

$$\ddot{\hat{x}} = -\hat{k}\hat{x} - \hat{\lambda}|\hat{x}|^{q-1}\hat{x} \tag{76}$$

$$\hat{E} = \frac{1}{2}\dot{\hat{x}}^2 + \frac{\hat{k}}{2}\hat{x}^2 + \frac{\hat{\lambda}}{q+1}|\hat{x}|^{q+1}\,. \tag{77}$$

which represents the oscillations of all moving particles of SPO2 albeit with different phases, according to the above definition.

Proceeding as in the previous subsection, we compute the SPO2 solution together with a neighboring orbit resulting from a small perturbation of the SPO2 initial conditions, and calculate the time evolution of their euclidean distance $D(t)$ for energies $E > 0$. As expected, $D(t)$ grows linearly at first until we reach a value $E = E_c(N)$, where it starts to grow exponentially, indicating that the SPO2 becomes unstable for $E > E_c(N)$. Plotting, as before, the values of the energy density $\mathcal{E} = E_c/N$ at which this first destabilization occurs vs. N, we find a similar result as with SPO1.

As demonstrated in Fig. 13 below, $\mathcal{E} = E_c/N$ for SPO2 also grows following a power law of the form $\mathcal{E} = a + bN^c$ with a $c > 0$ exponent, just as we found for the SPO1 orbit, given in this case by the expression

$$\mathcal{E}(N) = 4.1 + 0.01\ N^{3.6}\,. \tag{78}$$

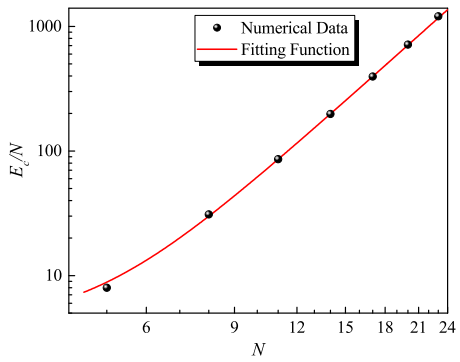

Fig. 13. Critical energy density graph for the SPO2 solution in a double logarithmic scale.

Comparing the power law graphs for the SPO1 and SPO2 solutions, (73) and (78) respectively, we observe first that they are qualitatively very similar. This offers added support to our earlier

argument that Hollomon systems may be in general more resilient as they become bigger, i.e. as their number of particles increase. Of course, this would have to be substantiated by carrying out a similar analysis for other SPOs, but the fact that it holds already for SPO1 and SPO2 is encouraging.

An additional conclusion that may also be drawn from the above results, is that the SPO2 orbit has a much higher destabilization threshold than SPO1, for all N, which is also the opposite than what we encountered in the FPU lattice where, as explained in the previous chapter, it takes more energy to destabilize SPO1 than SPO2!

IV. CONCLUSIONS

At the beginning of this thesis, I presented an introduction to the class of dynamical systems called N degree of freedom Hamiltonian systems and mentioned their importance in studying a wide variety of physical ptoblems. First I reviewed the cases of N=1 and N=2 degrees of freedom, using as examples a simple linear harmonic oscillator, all of whose solutions are periodic with the same frequency ω around a single stable fixed point. Proceeding then to a 1-degree of freedom simple pendulum equation, I remarked that its nonlinearity allows for the presence of two equilibrium points one stable and one unstable. Around the stable one, we observed again a region filled with periodic solutions but this time with a frequency that depends on the choice of initial conditions.

I then proceeded to discuss a *linear Hamiltonian system of N=2 degrees of freedom* possessing two integrals of the motion and describing two equal masses connected to each other (and each tied to a right and a left wall repectively) by harmonic springs of equal spring constant. I explained how we obtain oscillations of two frequencies for their motion, ω_1 and ω_2, yielding closed (periodic) orbits on 2-dimensional invariant tori only if the ratio of frequencies ω_1/ω_2 is rational, otherwise the orbits never close on these tori and are called quasiperiodic.

Next, I introduced the concept of Poincare's surface of section with regard to the famous non-integrable Henon-Heiles Hamiltonian, which shows very clearly the dynamics of simple periodic orbits (SPOs) under different levels of total energy E. Indeed, increasing the energy to $E = 1/8$ allows us to see widespread chaotic regions, except at places where there are still stable SPOs. Thus, all the way to the escape energy $E = 1/6$ we see that the destabilization of SPOs leads to the growth of chaotic regions, until they extend over most of the available energy surface. Above $E = 1/6$, almost all orbits escape to infinity.

Thus, to study such phenomena in many particle systems of interest to Statistical Mechanics, we described studies of other researchers on the N-degree of freedom Fermi Pasta Ulam (FPU) model of coupled nonlinear oscillators, which have led to the following important observations:

1) It is useful to know the energy values $E_c(N) > 0$ at which some fundamental SPO first become unstable, since for $E > E_c(N)$ the chaotic regions around the SPOs will be either "large" or "small", depending on the relative magnitudes of these thresholds $E_c(N)$.
2) In particular, it was found that, as N increases indefinitely, the unstable SPOs are surrounded by thin layers of "weak chaos" or large regions of "strong" chaos, depending on whether the SPO satisfies $E_c(N) \to 0$ as $E_c(N) \approx 1/N^\alpha$, where $\alpha = 2$ or $\alpha = 1$ respectively.

In the third chapter of the thesis, I turned to new results obtained recently studying the same questions as above for another class of N-degree of freedom Hamiltonian systems describing a 1-dimensional lattice of so-called Hollomon oscillators. These oscillators are very important in nonlinear elasticity, since beside harmonic (quadratic) terms they include in their potential nonlinearities of fractional power $1 < \mu = 4n/(2n+1) < 2, n = 1, 2, ...$ Choosing $\mu = 4/3$ in our studies, our results for the Hollomon SPO1 orbits show that the lattice does not change its behavior at low energies, as exemplified by the SPO1 oscillations that remain stable even for large energy intervals $0 < E < E_c(N)$. In fact, the threshold energy density values $\mathcal{E} = E_c(N)/N$ for SPO1 *grow* following a power law $\mathcal{E} \sim N^c$ with positive exponent $c = 2.82$ as the total number of particles N increases indefinitely.

This result is contrary to what has been obtained for Fermi-Pasta-Ulam lattices and seems to be a direct consequence of the particular physical properties of Hollomon's elasticity law. Performing a similar study of the behavior of $\mathcal{E} = E_c(N)/N$ vs. N for another important solution called SPO2, we find analogous results, where the exponent of N is even larger, i.e. $c = 3.6$, for this oscillatory mode. Thus, we conclude that if similar results as we have found for SPO1, SPO2, hold for many

other such orbits then it may indeed be true that elastic materials obeying Hollomon's law, become more stable and resilient, as their size increases.

REFERENCES

[1] Ch. Antonopoulos, and T. Bountis. *Stability of simple periodic orbits and chaos in a Fermi-Pasta-Ulam lattice*. Phys. Rev.E vol. 73, pp. 56-206. (2006).

[2] Ch. Antonopoulos, T.C. Bountis, and Ch. Skokos. *Chaotic dynamics of N-degree of freedom Hamiltonian systems*. Int. J. Bifurcat. Chaos, vol. 16, pp. 1777-1793. (2006).

[3] V.I. Arnold. *Mathematical Methods of Classical Mechanics*. Springer, New York (1989).

[4] G.P. Berman and F.M. Izrailev. *The Fermi-Pasta-Ulam problem: Fifty years of progress*. Chaos, vol. 15, 015104 (2005).

[5] T. Bountis, and H. Skokos. *Complex Hamiltonian Dynamics*. Springer Science & Business Media, vol. 10. (2012).

[6] N. Budinsky and T. Bountis, Physica D **8**, 445 (1983).

[7] F. D. Burgoyne. *Generalized trigonometric functions*. Mathematics of Computation, vol. 18, pp. 314-316. (1964).

[8] B.V. Chirikov. *A universal instability of many-dimensional oscillator systems*. Phys. Rep., vol. 52, pp.263–379 (1979).

[9] R.M. Conte and M.Musette. *The Painleve Handbook*. Springer, Heidelberg (2008).

[10] G. Contopoulos. *Order and Chaos in Dynamical Astronomy*. Springer, Heidelberg (2002).

[11] H.T. Davis. *Introduction to Nonlinear Differential and Integral Equations*. Dover, New York. (1962).

[12] J. De Luca, A.J. Lichtenberg. *Transitions and time scales to equipartition in oscillator chains: Low-frequency initial conditions*. Phys. Rev., vol. 66, 026206 (2002).

[13] J. De Luca, A.J. Lichtenberg, M.A. Lieberman. *Time scale to ergodicity in the Fermi-Pasta-Ulam system*. Chaos, vol. 5, pp. 283–297 (1995).

[14] S. Flach, M.V. Ivanchenko, O.I. Kanakov. *q-Breathers and the Fermi-Pasta-Ulam problem*. Phys. Rev. Lett., vol. 95, 064102 (2005).

[15] J. Ford. *The Fermi-Pasta-Ulam problem: Paradox turns discovery*. Phys. Rep., vol. 213, pp. 271–310 (1992).

[16] A. Goriely. *Integrability and Nonintegrability of Dynamical Systems*. World Scientific, Singapore (2001).

[17] M. Hénon, C. Heiles. *The applicability of the third integral of motion: some numerical experiments*. Astron. J., vol. 69, pp. 73–79 (1964).

[18] E. Hille. *Lectures on Ordinary Differential Equation*. Addison-Wesley, Reading, Mass. (1969).

[19] J.H. Hollomon. *Tensile deformation*. Aime Trans, vol. 12, no. 4, pp. 1-22. (1945).

[20] A.J. Lichtenberg, and M.A. Lieberman. *Regular and Chaotic Dynamics*. Second edition. Springer, New York. (1992).

[21] P. Lindqvist. *Note on a nonlinear eigenvalue problem*. Rocky Mountain J.Math., vol. 23, pp. 281-288. (1993).

[22] A.M. Lyapunov. *The General Problem of the Stability of Motion*. Taylor and Francis, London. (1992) *(English translation from the French: Liapounoff, A.: Problème général de la stabilité du mouvement. Annal. Fac. Sci. Toulouse 9, 203-474 (1907). The French text was reprinted in Annals Math. Studies Vol.17 Princeton Univ.Press (1947). The original was published in Russian by the Mathematical Society of Kharkov in 1892)*.

[23] T. Manos, Ch. Skokos, E. Athanassoula, T. Bountis. *Studying the global dynamics of conservative dynamical systems using the SALI chaos detection method*. Nonl. Phen. Compl. Syst. vol. 11, pp. 171-176. (2008).

[24] E. Mitsokapas. *A Class of Hamiltonian Systems with Fractional Power Nonlinearities*. Erasmus Student Report, Nazarbayev University. (2017).

[25] N. Ooyama, H. Hirooka, and N. Saitô, J. Phys. Soc. Jpn. **27**, 815 (1969).

[26] P. Panagopoulos, T.C. Bountis, Ch. Skokos. *Existence and stability of localized oscillations in 1-dimensional lattices with soft spring and hard spring potentials*. J. Vib. Acoust. vol. 126, pp. 520-527. (2004).

[27] L. Perko. *Differential Equations and Dynamical Systems*. Springer, New York. (1995).

[28] A. Ramani, B. Grammaticos, T. Bountis. *The Painlevé property and singularity analysis of integrable and non-integrable systems*. Phys. Rep., vol. 180, pp. 159–245 (1989).

[29] D. Shelupsky. *A generalization of the trigonometric functions*. The American Mathematical Monthly, vol. 66, no. 10, pp. 879-884. (1959).

[30] Ch. Skokos. *Alignment indices: A new, simple method for determining the ordered or chaotic nature of orbits*. J. Phys. AMath. Gen., vol. 34, pp. 10029-10043. (2001).

[31] Ch. Skokos. *The Lyapunov characteristic exponents and their computation*. Lect. Notes Phys. 790, pp. 63-135. (2010).

[32] Ch. Skokos, T. Bountis, and CH. Antonopoulos. *Geometrical properties of local dynamics in Hamiltonian systems: The generalized alignment index (GALI) method*. Physica D231, pp. 30-54. (2007).

[33] D. Wei, andv Yu Liu. *Some generalized trigonometric sine functions and their applications*. (2012).

[34] S. Wiggins. *Applied Nonlinear Dynamical Systems and Chaos*. Springer, New york. (1990).